REGIONAL SEISMIC EVENT CHARACTERIZATION USING A BAYESIAN KRIGING APPROACH

Mark Fisk and Steven Bottone, Mission Research Corporation
Gary McCartor, Southern Methodist University

Sponsored by U. S. Department of Defense
Defense Threat Reduction Agency

Contract No. DSWA01-98-C-0152

ABSTRACT

This effort focuses on collecting and analyzing regional seismic data for earthquakes and underground explosions to improve seismic event characterization capabilities with regard to monitoring the Comprehensive Nuclear-Test-Ban Treaty (CTBT). Digital data have now been acquired and processed for 267 regional recordings of 160 underground nuclear (UNE) and chemical (UCE) explosions. The explosion data set includes 99 Nevada Test Site (NTS) UNE's recorded by MNV and KNB; 6 Lop Nor UNE's recorded by NIL, ZAL, ULN, WMQ, BRVK and MAKZ; 22 Semipalatinsk (STS) UNE's recorded by WMQ and BRVK; 6 Novaya Zemlya (NZ) UNE's recorded by ARCES and KEV; and one UNE at the Indian Test Site recorded by NIL. In addition, the set includes 20 Former Soviet Union (FSU) peaceful nuclear explosions (PNE) recorded by BRVK and KEV; and 6 STS UCE's recorded by ZAL and BRVK. (Note: not all of these explosions have recordings by all stations listed.) Over 5300 regional recordings, between 3 and 17 degrees, by existing seismic stations of the International Monitoring System (IMS) are also used in this study. The regional recordings correspond to 4173 presumed earthquakes above mb 3.5 in the Reviewed Event Bulletin (REB) that were processed at the prototype International Data Center (pIDC). Maximum amplitude measurements of Pn, Pg, Sn and Lg have been computed in several frequency bands ranging from 2 Hz up to 14 Hz (depending on the Nyquist frequency of a given station).

The data for the presumed earthquakes have been used to estimate attenuation corrections for Pn/Sn and Pn/Lg amplitude ratios in the 2–4, 4–6, 6–8, and 8–10 Hz passbands for tectonic and stable region types. The regional phase amplitude ratios are further corrected for path variations using a Bayesian Kriging algorithm. A correction surface is determined for each type of amplitude ratio at each station as an optimal linear combination of existing amplitude-ratio data at the station, giving greater weight to data nearer to the location of the event to be corrected. A corresponding uncertainty surface is also estimated in terms of the residual variance of the data and a calibration variance. For well-calibrated locations, the correction converges to the mean of nearby data and the uncertainty converges to the residual variance. For locations far from calibration data, the correction surface converges to the worldwide average, with larger uncertainty due to both residual and calibration variances.

Using these correction and uncertainty surfaces, corrected values of Pn/Smax(6–8 Hz) are then used to define a hypothesis test that fixes the significance level with respect to misclassifying explosions. A score is computed for each event such that events with negative scores are not screened out at the specified significance level. The significance level used here has been set such that none of the available underground explosions are screened out. Events with scores greater than zero are screened out (i.e., are considered to be inconsistent with the hypothesis that the event belongs to the explosion population). Screening rates for earthquakes above mb 3.5 are estimated and improvements in event characterization performance due to Kriging are demonstrated.

OBJECTIVE

This effort focuses on collecting and analyzing regional seismic data for underground explosions and earthquakes to improve seismic event characterization capabilities with regard to monitoring the Comprehensive Nuclear-Test-Ban Treaty (CTBT). Key aspects of this effort include: (i) acquiring regional seismic recordings for underground explosions and earthquakes; (ii) processing the waveforms to measure Pn, Pg, Sn and Lg amplitudes in various frequency bands; (iii) evaluating optimum processing techniques for regional amplitude ratios; (iv) developing a regional event-screening capability, which includes establishing necessary region-specific training sets and distance corrections; and (v) evaluating optimum screening criteria for various regions and comparing explosion and earthquake characteristics in an effort to understand how regional event characterization parameters and screening criteria can be transported to regions for which no explosion data exist.

This work is motivated by the fact that, although depth and Ms:mb are essential methods in the characterization of seismic events, the experimental depth and Ms:mb screening criteria being tested at the prototype International Data Center (pIDC) currently screen out less than 50% of the presumed earthquakes above mb 3.5 in the Reviewed Event Bulletin (REB) (e.g., Fisk et al., 1999b). However, there are a significant number of events in the REB with regional seismic data that can provide additional event-screening performance. Many studies have indicated that ratios of high-frequency, regional seismic phase amplitude ratios can provide adequate separation between underground explosions and earthquakes to aid in monitoring the CTBT (see Fisk et al., 1996, and references therein).

We describe data that have been compiled and processed for 267 regional recordings of 160 underground explosions. These explosions are compared to over 5300 regional waveforms, recorded by existing seismic stations of the International Monitoring System (IMS), for 4173 presumed earthquakes, above mb 3.5, processed at the pIDC. After applying distance corrections that depend on region type (tectonic or stable) to Pn/Sn and Pn/Lg ratios, a Bayesian Kriging algorithm is applied at each station to further correct for path variations. The Kriging algorithm also provides a corresponding uncertainty surface. To characterize the events, we use Pn/Smax in the 6–8 Hz band, where Smax = max(Sn,Lg), which has been corrected for distance and for path variations using the Kriged surface. We apply a hypothesis test, which accounts for the varying uncertainty associated with the Kriged surface, to these data sets to assess whether an event is consistent with the explosion population at a fixed significance level with respect to incorrectly screening out an explosion. A *score* is computed such that events with positive scores are screened out, i.e., are inconsistent with the hypothesis that the event belongs to the explosion population. Events with scores less than or equal to zero are not screened out. At the 0.005 significance level, none of the available explosions are screened out.

RESEARCH ACCOMPLISHED

Regional Explosion Data

We have compiled 267 regional seismic recordings for 160 underground nuclear (UNE), chemical (UCE) and peaceful nuclear (PNE) explosions. Table 1 summarizes our current database of regional explosion recordings, which represent explosions in diverse geological regions at various test sites. These explosions cover a magnitude range of about ML 2.4 to mb 6.2, and a distance range of about 2 to 17 degrees. The regional measurements for the NTS explosions recorded by MNV and KNB were provided by LLNL (Patton and Walter, 1994) and the PNE data recorded by BRVK were provided by Jack Murphy (1998).

The processed data consist of regional phase amplitudes, Pn, Pg, Sn and Lg in the 2–4, 4–6, 6–8, and 8–10 Hz bands. Not all events have complete sets of amplitude ratios. Six of the UNE's conducted on Novaya Zemlya (NZ) were recorded by station KEV and three were recorded by ARCES. Six UNE's occurred at the Lop Nor test site, one recorded by ZAL, four by NIL, two by ULN, one by WMQ, four by BRVK and four by MAKZ. Semipalatinsk (STS) provides 22 UNE's, 21 recorded by WMQ and six by BRVK. There is one UNE at the Indian Test Site recorded by NIL. There are 99 explosions from the Nevada Test Site (NTS), 84 of which have recordings at both MNV and KNB, nine at MNV only, and six at KNB only. In addition, the set includes 20 Former Soviet Union (FSU) PNE's, 16 recorded by BRVK and six by KEV; and 6 STS UCE's, five recorded by ZAL and six by BRVK. A few events in the table do not have either Pn/Sn(6–8 Hz) or Pn/Lg(6–8 Hz) available, and therefore not are used in the screening test described below.

Table 1: Summary of Regional Underground Nuclear Explosion Data

Station	Distance	Magnitude	Test Site	Explosion Dates
KEV	9.4 3.1–19.5	5.52–5.90 4.70–5.50	NZ UNE's FSU PNE's	821011, 841025, 870802, 880507, 881204, 901024 5 (820904–850718)
ARCES	9.9	5.60–5.90	NZ UNE's	880507, 881204, 901024
ZAL	12.2 6.2, 5.5, 5.5 6.0, 6.0	4.71 3.95, n/a, n/a, 3.80, 3.67	Lop Nor UNE STS UCE's	960729 970803, 970831, 970928, 980822, 990925
NIL	14.4–14.7 6.7	5.73, 5.54 5.69, 4.71 5.00	Lop Nor UNE's India UNE	950515, 950817, 960608, 960729 980511
ULN	14.3	5.73, 5.54	Lop Nor UNE's	950515, 950817
WMQ	8.6 2.2	4.6–6.1 4.7	STS UNE's Lop Nor UNE	21 (870606–891004) 880929
BRVK	16.8–16.9 6.2 5.8–6.2 7.2–17.2	6.00,5.73 5.54, 5.69 5.70–7.20 3.95, n/a, n/a, 3.80, n/a, 3.67 4.5–5.8	Lop Nor UNE's STS UNE's STS UCE's FSU PNE's	941007, 950515, 950817, 960608 6 (88023–881217) 970803, 970831, 970928, 980822, 980917, 990925 16 (730815–880906)
MAKZ	6.9–7.2	6.00, 5.73, 5,69, 4.71	Lop Nor UNE's	941007, 950515, 960608, 960729
MNV	1.7–2.2	2.4–5.5	NTS UNE's	93 (1979–1992)
KNB	2.5–2.8	2.6–5.5	NTS UNE's	90 (1979–1992)

Regional Earthquake Data

Over 5300 regional waveforms that were recorded by 52 IMS seismic stations and processed at the pIDC are used in this study. These recordings correspond to 4173 distinct REB events above mb 3.5 that are presumed to be earthquakes. The restriction to mb > 3.5 is used to reduce the possibility of mining blasts contaminating the earthquake data sets. We also limit the events to those with distances beyond 3 degrees to avoid problems of distinguishing Pn and Pg, and to those less than 17 degrees, although regional phase amplitudes are computed at distances up to 20 degrees at the pIDC. In addition, we limit this study to data from IMS stations that have at least 20 or more recordings so that useful training sets may be formed. Figure 1 shows the locations of the 4173 presumed earthquakes and the 160 explosions used in this study. The locations of the 52 IMS stations and 4 non-IMS stations (KEV, WMQ, BRVK and KNB) are included.

Maximum amplitudes of Pn, Pg, Sn and Lg have been measured at the pIDC in the 2–4, 4–6, 6–8, 8–10 and 10–12 Hz bands (depending on the Nyquist frequency of the instrument). For this study, we use Pn/Sn and Pn/Lg in the 6–8 Hz bands that satisfy the signal-to-noise criteria of Pn signal divided by pre-Pn noise greater than 2.0 and S signal divided by pre-S noise greater than 1.2.

In addition to the pIDC data, the earthquake data set also includes 60 recordings by MNV and 75 by KNB of Pn/Lg in the 4–6, 6–8, and 8–10 Hz bands for earthquakes near NTS, processed by LLNL in the same way as the 99 UNE's. These earthquakes are necessary to properly calibrate stations MNV and KNB.

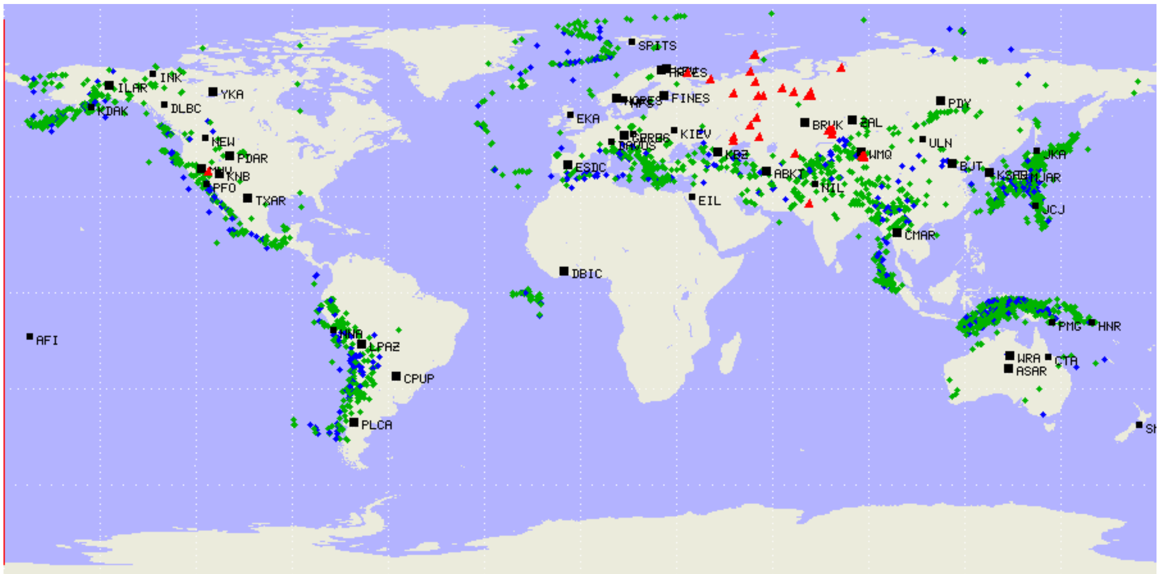

Figure 1. Locations of 160 nuclear explosions (triangles) and 4173 REB earthquakes with mb 3.5 and above. Locations of 52 IMS stations and 4 stations with explosion recordings (KEV, WMQ, BRVK, and KNB) are also shown.

Distance Corrections

The unequal rates of attenuation with distance between regional P and S phases necessitate a correction for distance if amplitude ratios recorded at different distances are to be compared (see Sereno, 1990, Bottone et al., 1997, Fisk et al., 1998, Fisk et al., 1999a and Fisk et al., 2000). P/S distance dependence is modeled by a three-parameter equation of the form

$$\log(\mathrm{P/S}) = a + b \log \Delta + c\Delta \,, \tag{1}$$

where a, b, and c are parameters depending on the particular amplitude ratio (Pn/Lg or Pn/Sn), frequency band and region type. Δ is the epicentral distance. Following Jenkins et al. (1998), we divide the world into tectonic and stable region types and estimate the three coefficients for each region type. We then correct all amplitude ratios at a given station using equation (1) with coefficients estimated using all data located in the appropriate region type. At this point we do not make station-dependent corrections; station dependence will result from Kriging. Figure 2 plots the distance dependence of all REB earthquakes in both the tectonic and stable regions for Pn/Lg(6–8 Hz) and Pn/Sn(6–8 Hz).

Bayesian Kriging

Corrections of regional amplitude ratios using worldwide distance corrections do not depend on station and do not take into account any variations in propagation amplitude that may depend on path differences. One way of treating path variations is Kriging. Kriging has been used to reduce the variance of regional amplitude ratios for earthquake populations (Fan et al., 1999, Rodgers et al., 1999). Ordinary Kriging provides a minimum-mean-square-error prediction (of, in our case, a regional amplitude ratio measured at a particular station) at a given spatial location that is an unbiased linear combination of previously measured data at N separate locations (Cressie, 1993). In Ordinary Kriging the prediction at an unobserved point that is located far from any data points converges to the mean of the available data at that station. For a station that has only data in a subregion with anomalous propagation properties, a prediction in another subregion far removed from this data may be incorrect. In such a subregion we wish for the prediction to converge to a value that is the average over all stations worldwide of the same region type. To achieve this limiting behavior, we generalize the Ordinary Kriging approach using Bayesian methods.

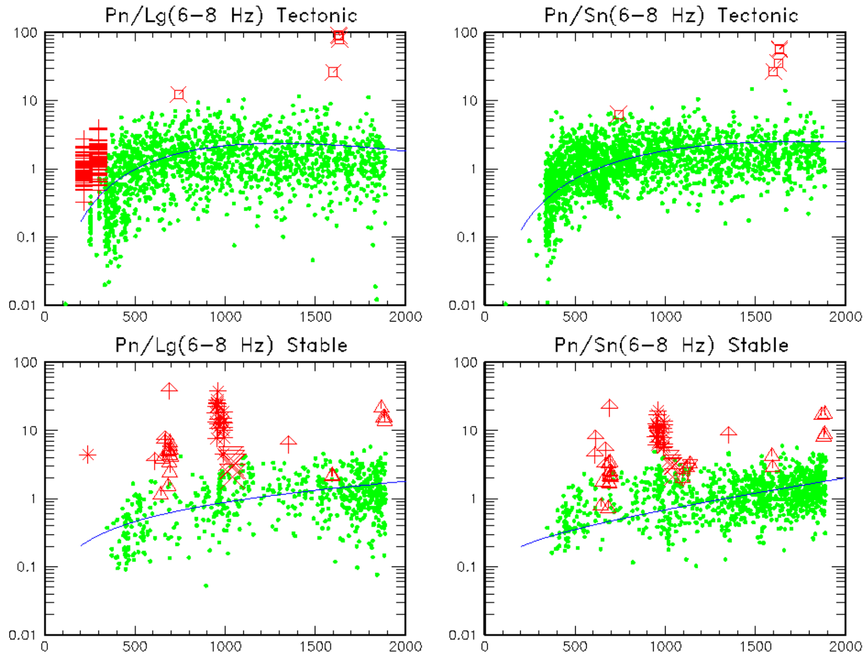

Figure 2. Uncorrected Pn/Lg(6–8 Hz) and Pn/Sn(6–8 Hz) versus distance in km for all REB events and explosions worldwide in tectonic and stable regions. The solid curves are best-fit, three-parameter estimates of the distance dependence for earthquakes.

Suppose we have *N* data values at locations, $\mathbf{s}_1,\ldots,\mathbf{s}_N$ for a particular regional amplitude ratio, say Pn/Sn(6–8 Hz), recorded by a single station. Let $\mathbf{x} = (x_1,\ldots,x_N)'$ be an *N*-dimensional data vector where the x_i, $i = 1,\ldots,N$, are distance-corrected values of log(P/S), where the distance corrections are relative to the worldwide wide average distance dependence, estimated by using P/S values for data available from all stations. We normalize the data so that the distance-corrected worldwide average is zero.

We assume that data at a given location, $\mathbf{s}_i$, can be modeled by a random variable with a normal distribution, with unknown mean, μ_i, and fixed variance (to be determined), σ_{r}^2, where σ_{r}^2 is the same at all locations, that is,

$$x_i \sim N(\mu_i, \sigma_{\mathrm{r}}^2) . \qquad (2)$$

We also assume that the means of the normal distributions at each location, μ_i, are also normally distributed random variables with zero mean, equal variances, σ_{c}^2, (to be determined), and correlation between any two μ_i and μ_j dependent only on the distance separating the two locations, that is,

$$\rho_{ij} = \mathrm{corr}(\mu_i, \mu_j) = f(\Delta(\mathbf{s}_i, \mathbf{s}_j)) , \qquad (3)$$

where $\Delta(\mathbf{s}_i, \mathbf{s}_j)$ is the epicentral distance between locations $\mathbf{s}_i$ and $\mathbf{s}_j$. The function *f* must be a positive definite function (function of positive type), ensuring that the covariance matrix of the random vector of means is positive definite. The form of this function is usually taken to be a known positive definite function with unknown parameters estimated using the available data. We generally use

$$f(\Delta) = \exp(-\Delta/\alpha) , \qquad (4)$$

where α, the correlation length, is estimated using the data.

We wish to determine an optimal predictor for the mean of an unobserved value located at $\mathbf{s}_0$ given the N data values, **x**, located at $\mathbf{s}_1,\ldots,\mathbf{s}_N$. We wish to determine the distribution, $p(\mu_0 \mid \mathbf{x})$, of the unknown mean, μ_0, at the unobserved location, $\mathbf{s}_0$, given the data, **x**. The expected value of this distribution (i.e., the posterior Bayes estimator) could be used as the estimator of μ_0 at that location. Under our assumptions we know $p(x_0,\mathbf{x} \mid \mu_0,\boldsymbol{\grave{\imath}})$ and $p(\mu_0,\boldsymbol{\grave{\imath}})$, where $\boldsymbol{\grave{\imath}} = (\mu_1,\ldots,\mu_N)'$, so we can use Bayes theorem to calculate $p(\mu_0 \mid \mathbf{x})$. Performing the appropriate integrals we get

$$p(\mu_0 \mid \mathbf{x}) \propto \int [\int p(x_0,\mathbf{x} \mid \mu_0,\boldsymbol{\grave{\imath}})\,dx_0]\; p(\mu_0,\boldsymbol{\grave{\imath}})\,d\boldsymbol{\grave{\imath}}\,. \tag{5}$$

Since integrals of normal distributions are normal distributions, $p(\mu_0 \mid \mathbf{x})$ will also be normally distributed, so the proportionality constant need not be determined explicitly. Substituting the appropriate distributions for $p(x_0,\mathbf{x} \mid \mu_0,\boldsymbol{\grave{\imath}})$ and $p(\mu_0,\boldsymbol{\grave{\imath}})$ as described above and performing the integral over x_0 gives

$$p(\mu_0 \mid \mathbf{x}) \propto \int_{-\infty}^{\infty} \exp\left[-\frac{1}{2}(\mathbf{y}-\boldsymbol{\acute{\imath}})' A_1 (\mathbf{y}-\boldsymbol{\acute{\imath}})\right] \exp\left[-\frac{1}{2}\boldsymbol{\acute{\imath}}'\Sigma^{-1}\boldsymbol{\acute{\imath}}\right] d\boldsymbol{\grave{\imath}}\,, \tag{6}$$

where **y** and $\boldsymbol{\acute{\imath}}$ are (N+1)-dimensional vectors given by $\mathbf{y} = (0,\mathbf{x}')'$ and $\boldsymbol{\acute{\imath}} = (\mu_0,\boldsymbol{\grave{\imath}}')'$, A_1 is an (N+1)-by-(N+1)-dimensional matrix given by

$$A_1 = \frac{1}{\sigma_{\mathrm{r}}^2}\begin{bmatrix} 0 & \mathbf{0} \\ \mathbf{0} & I_N \end{bmatrix}, \tag{7}$$

where I_N is the identity matrix in N dimensions, and Σ is an (N+1)-by-(N+1)-dimensional covariance matrix such that

$$\Sigma_{ij} = \sigma_{\mathrm{c}}^2 \rho_{ij}\,, \qquad i,j = 0,1,\ldots,N\,. \tag{8}$$

The integral in equation (6) can be shown to be proportional to

$$p(\mu_0 \mid \mathbf{x}) \propto \int_{-\infty}^{\infty} \exp\left[-\frac{1}{2}(\boldsymbol{\acute{\imath}}-\tilde{\boldsymbol{\grave{\imath}}})' S^{-1} (\boldsymbol{\acute{\imath}}-\tilde{\boldsymbol{\grave{\imath}}})\right] d\boldsymbol{\grave{\imath}}\,, \tag{9}$$

where

$$S^{-1} = \Sigma^{-1} + A_1 \tag{10}$$

and

$$\tilde{\boldsymbol{\grave{\imath}}} = S\,A_1\,\mathbf{y}\,. \tag{11}$$

This integral is easily computed by using the theorem that if a random vector, $\boldsymbol{\acute{\imath}}$, is distributed as $N(\tilde{\boldsymbol{\grave{\imath}}},S)$, then the marginal distribution of any set of components of $\boldsymbol{\acute{\imath}}$ is multivariate normal with means, variances, and covariances obtained by taking the corresponding components of $\tilde{\boldsymbol{\grave{\imath}}}$, and S. This gives

$$p(\mu_0 \mid \mathbf{x}) \propto \exp\left[-\frac{1}{2}(S_{00})^{-1}(\mu_0-\tilde{\mu}_0)^2\right], \tag{12}$$

or, equivalently, μ_0, given **x**, is distributed as the normal, $N\left(\tilde{\mu}_0,\sigma^2\right)$, where

$$\tilde{\mu}_0 = (S\,A_1\,\mathbf{y})_0 \tag{13}$$

and

$$\sigma^2 = S_{00} = [(\Sigma^{-1} + A_1)^{-1}]_{00}\,. \tag{14}$$

A prediction surface, which can also serve as a correction surface, is obtained by computing $\tilde{\mu}_0(\mathbf{s}_0)$ for all values of $\mathbf{s}_0$ within regional distances of the station. An uncertainty surface is given by $\sigma^2(\mathbf{s}_0)$. In principle, such surfaces can be obtained for both earthquakes and explosions at each station, however, due to the scarcity of explosion data, only earthquake surfaces are practical.

An explosion data value, say Pn/Sn(6–8 Hz), at location $\mathbf{s}_0$, can be compared to the earthquake surface by computing the difference $x(\mathbf{s}_0) - \tilde{\mu}_0(\mathbf{s}_0)$. This should be a large positive number if explosions are to be distinguished from earthquakes. Any unknown event at $\mathbf{s}_0$ can also be compared to the surface in the same way, however, if we wish to compare any of the *N* earthquakes used to determine the surface with a prediction at that location, we must remove that earthquake from the data set and compute a new surface value at that location using the *N*–1 remaining earthquakes (the leave-one-out procedure). There are three parameters that must be estimated using all available data, σ_c^2, the calibration variance, σ_r^2, the residual variance, and α, the correlation length. Preliminary work suggests that α is typically about 6 degrees, and that σ_c^2 and σ_r^2 are about equal, their sum being equal to the total variance of the data.

Figure 3 shows a typical correction surface at station NIL for distance-corrected log[Pn/Sn(6–8 Hz)], with the corresponding uncertainty surface shown in Figure 4. At locations far from available data, the surface approaches the distance-corrected worldwide average. The locations of nuclear explosions and earthquakes recorded by NIL are depicted by triangles and crosses, respectively. White markers indicate values that are less than the surface, while black markers indicate that the value is greater than the surface. The size of the marker is proportional to the absolute value of the distance from the surface. Thus, very explosion-like values correspond to large black triangles. Figure 4 shows that the uncertainty is lower in areas containing many data points, while it is higher in areas around NIL that are relatively aseismic.

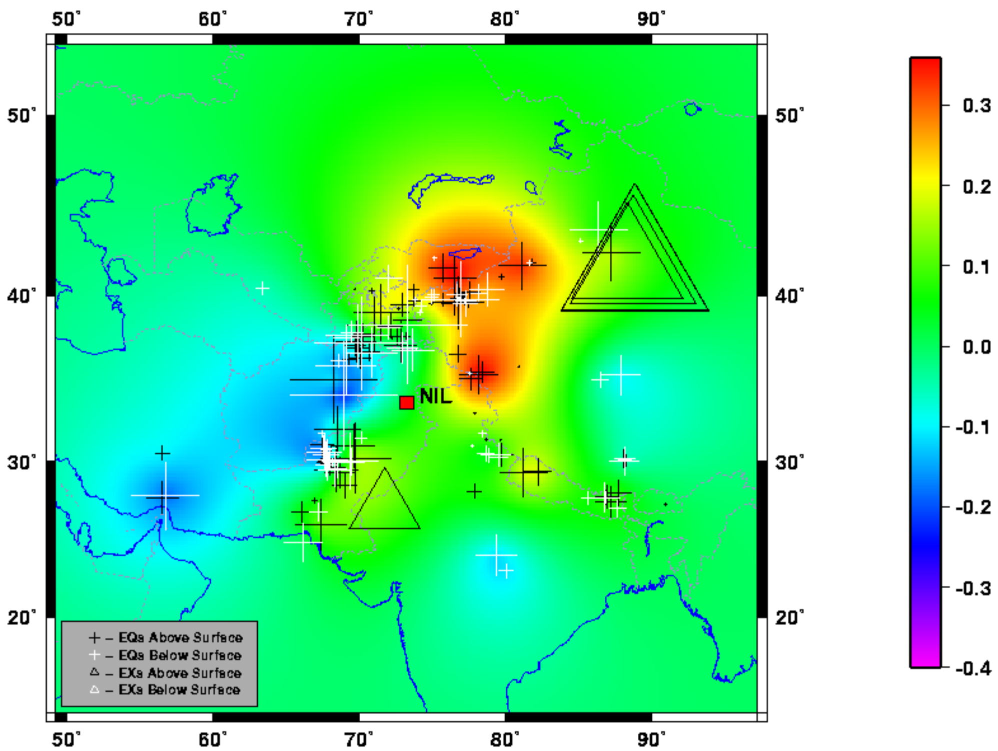

Figure 3. Bayesian Kriged surface for log[Pn/Sn(6–8 Hz)] at NIL. Triangles show locations of nuclear explosions and crosses show the locations of earthquakes. Black (white) markers have values above (below) the surface. Markers size is proportional to the absolute distance from the surface.

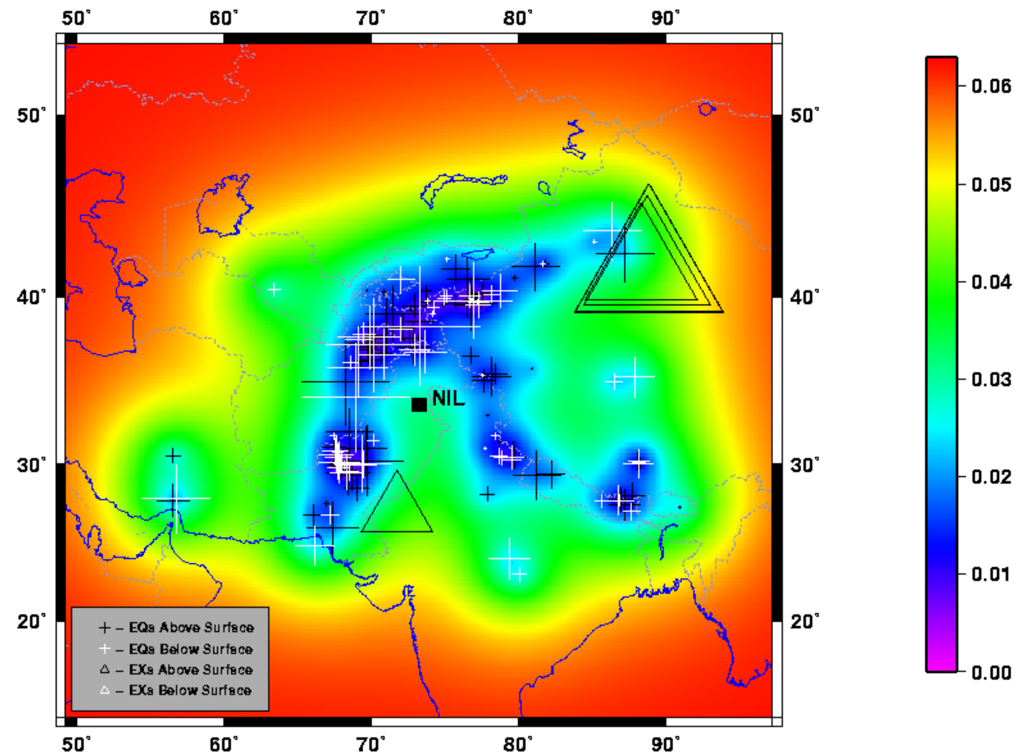

Figure 4. Uncertainty (variance) surface for log[Pn/Sn(6–8 Hz)] at NIL. Triangles show locations of nuclear explosions and crosses show the locations of earthquakes. The markers are the same as Figure 3.

Event-Screening Criterion and Score

An event-screening criterion can be developed from a hypothesis test, using the corrected data and the associated uncertainty, that has a fixed significance level with respect to screening out an explosion. For each station, correction surfaces are calculated for both log[Pn/Sn(6–8 Hz)] and log[Pn/Lg(6–8 Hz)], as well as uncertainty surfaces. To construct a hypothesis test, we define a scaled variable, λ, given by

$$\lambda = \frac{y - \mu_{\mathrm{EX}}}{\sqrt{\sigma^2 + \sigma^2_{\mathrm{r,EQ}}}}\,, \tag{15}$$

where

$$y = x(\mathbf{s}_0) - \tilde{\mu}_0(\mathbf{s}_0)\,. \tag{16}$$

In Equations (15) and (16), $x(\mathbf{s}_0)$ is the distance-corrected value of log[Pn/Smax(6–8 Hz)] for a test event located at $\mathbf{s}_0$, where Pn/Smax is Pn/Sn if Sn is larger than Lg or Pn/Lg otherwise, $\tilde{\mu}_0(\mathbf{s}_0)$ is the correction surface value at $\mathbf{s}_0$ for Pn/Smax, μ_{EX} is the mean value of y for all explosions in the data set, σ^2 is the uncertainty surface value at $\mathbf{s}_0$, and $\sigma^2_{\mathrm{r,EX}}$ is the residual variance for explosions. If all assumptions are true, then λ should be normally distributed with mean zero and variance one. With this in mind, we define the screening criterion to be

$$\lambda < -z_{\alpha}\,, \tag{17}$$

where z_{α} is the (1-α)-percentile of the standard normal distribution, which we usually take as 2.576 for a 0.005 significance level. We also define a regional *score* such that an event is screened out at the α significance level if the score is greater than zero,

$$\text{Score}_R = -\frac{\lambda}{z_\alpha} - 1. \tag{18}$$

We have applied this screening criterion to 140 explosions and 4173 REB events above mb 3.5. For each explosion, the Kriged correction and uncertainty surface values are computed at the explosion location for each station with regional recordings, using all earthquakes available at that station. The value *y*, given by equation (2), is then computed, from which the mean, μ_{EX}, can be estimated. The explosion data is also used to estimate the explosion residual variance, $\sigma^2_{r,EX}$, which we estimate to be $(0.22)^2$. The other estimates used are $\sigma_c = 0.25$, $\sigma_{r,EQ} = 0.25$, and $\alpha = 6.0$ degrees. For each earthquake a Kriged and uncertainty surface is computed at the location of the earthquake by using the remaining earthquakes recorded at that station (using the leave-one-out procedure). The scaled value λ for each event is determined and a score for each event is computed. Those events with positive scores are screened out.

For our data set, none of the 140 explosions are screened out at the 0.005 significance level, while about 73% of the 4173 REB earthquakes are screened out. Figure 5 shows a plot of the scores for all of these earthquakes and explosions. For comparison, Figure 6 shows a plot of distance-corrected log[Pn/Smax(6–8 Hz)] for the same events, before the Kriged corrections were applied. As can be seen from Figure 6, if the explosion with the smallest amplitude ratio had been used as the screening threshold, only about 50% of the earthquakes would have been screened out, showing the improvement resulting from Kriging.

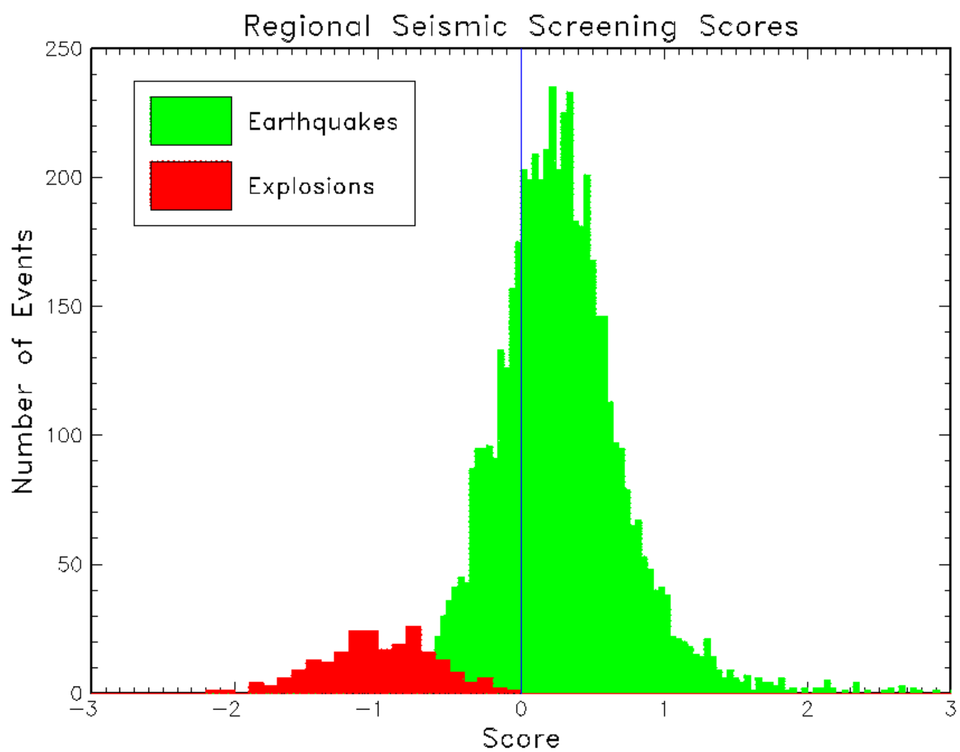

Figure 5. Histograms of regional screening scores for 140 explosions (left) and 4173 earthquakes (right). None of the explosions are screened out (all have scores less than zero using a significance level of 0.005), while 73% of the REB earthquakes are screened out (scores greater than zero).

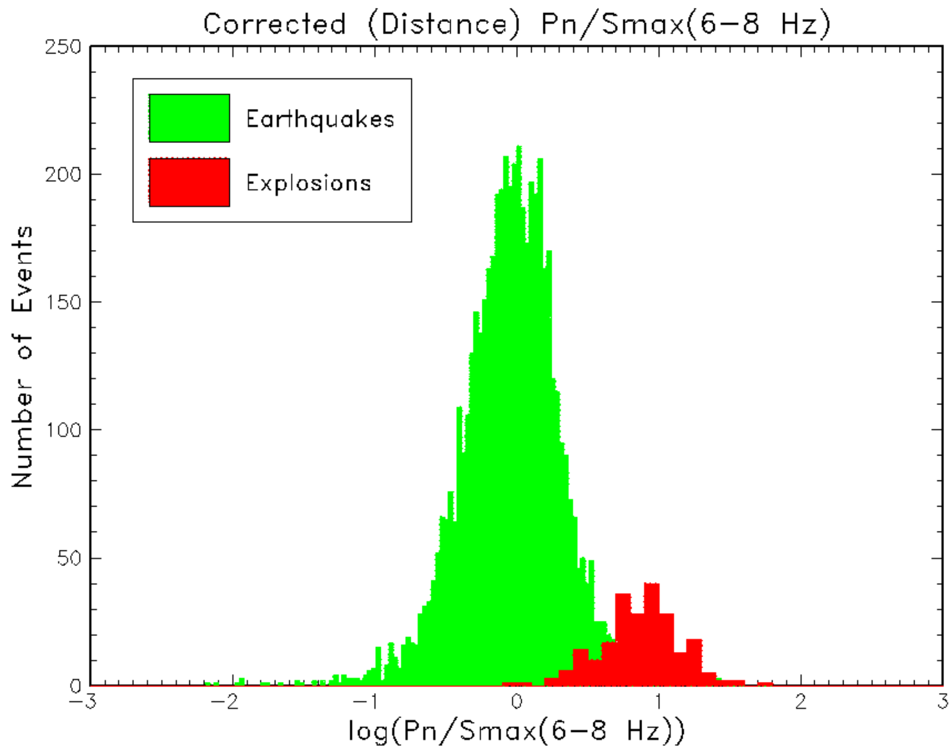

Figure 6. Histograms of log[Pn/Smax(6–8 Hz)] with worldwide distance corrections for 140 explosions (right) and 4173 earthquakes (left). If the explosion with the smallest value were used as a threshold only about 50% of the earthquakes would be screened out.

CONCLUSIONS AND RECOMMENDATIONS

High-frequency, regional seismic P/S amplitude ratios have potential utility to augment the seismic event-screening procedures based on event depth and Ms:mb. Screening performance is generally improved by correcting regional amplitude ratios using spatial techniques, which help account for path variations. In this paper we developed a Bayesian Kriging algorithm that treats subregional variations and accounts for local uncertainty in such a way that in regions far from any calibration data the correction surface approaches the worldwide average and the uncertainty surface approaches maximum uncertainty. Using the screening procedure described in this paper, no available underground explosions were screened out at the Nevada, Lop Nor, Semipalatinsk, Indian, or Novaya Zemlya test sites, while about 73% of REB events above mb 3.5 and with Pn-SNR > 2.0 and S-SNR >1.2 can be screened out, a great improvement over using worldwide distance corrections alone. This screening performance compares favorably with that of Ms:mb. The experimental depth and Ms:mb screening criteria at the pIDC currently screen out less than 50% of REB events above mb 3.5 and about 70% of REB events that have applicable regional data are relatively shallow and do not have an Ms measurement.

There are several potential ways to further improve the regional screening performance. The hypothesis test presented in this paper uses only one screening parameter, namely Pn/Smax(6–8 Hz). Extending the test to include additional amplitude ratios, e.g., Pn/Smax(4–6 Hz) and/or Pn/Smax(8–10 Hz), generally improves screening performance. Another method that may improve performance is multistation averaging, where amplitudes ratios for the same event recorded at more than one station are averaged before applying the hypothesis test. Currently, about 25% of all REB events with regional amplitudes have recordings at two stations or more, a percentage that will increase as more IMS seismic stations come online. Currently, the pIDC measures regional phase amplitudes only on vertical components. Although P/S ratios measured on vertical components show reasonable power for separating earthquakes from explosions, Kim et al. (1997) showed that P/S spectral ratios of rotated, three-component (3-C) records improve the power. Since most IMS seismic stations have 3-C broadband sensors, the horizontal components should also be considered for event characterization. Preliminary work is this area has shown promise.

Key Words: CTBT monitoring; regional seismic data; event characterization; underground explosions; Bayesian Kriging

REFERENCES

Bottone, S., M. D. Fisk, H. L. Gray, G. D. McCartor, and R. J. Carlson (1997). Initial Regionalization Efforts for the IMS Seismic Network, PL-TR-97-2090, Phillips Laboratory, Hanscom AFB, MA.

Cressie, N. (1993). *Statistics for Spatial Data*, Revised Edition, John Wiley and Sons, Inc., New York.

Fan, G.-W., T. Lay and S. Bottone (1999). Path corrections for source discriminants: A case study at two International Seismic Monitoring stations, submitted to *Pure and Applied Geophysics*.

Fisk, M. D., S. Bottone, R. J. Carlson, H. L. Gray, and G. D. McCartor (1998). Event Characterization Development and Analysis at the Prototype IDC, MRC-R-1548, Mission Research Corporation, Santa Barbara, CA, to appear as a DTRA technical report.

Fisk, M. D., S. Bottone, H. L. Gray, and G. D. McCartor (1999). Event characterization using regional seismic data, *Proceedings of the 21st Seismic Research Symposium*, 427-437.

Fisk, M. D., S. Bottone, and G. D. McCartor (2000). A Seismic Event-Screening Approach Using Regional P/S Amplitude Ratios, MRC-R-1603, Mission Research Corporation, Santa Barbara, CA, to appear as a DTRA technical report.

Fisk, M. D., H. L. Gray, and G. D. McCartor (1996). Regional discrimination without transporting thresholds, *Bull. Seism. Soc. Am.*, **86**, 1545-1558.

Fisk, M. D., D. Jepsen, and J. R. Murphy (1999). Experimental seismic event-screening criteria at the Prototype International Data Center, submitted to *Pure and Applied Geophysics*.

Jenkins, R. D., T. J. Sereno, and D. A. Brumbaugh (1998). Regional Attenuation at PIDC Stations and the Transportability of the S/P Discriminant, AFRL-VS-HA-TR-98-0046, Air Force Research Laboratory, Hanscom Air Force Base, MA.

Kim, Y. K., V. Aharonian, A. L. Lerner-Lam and, P. G. Richards (1997). Discrimination of earthquakes and explosions in southern Russia using regional high-frequency three-component data from IRIS/JSP Caucasus Network, *Bull. Seism. Soc. Am.*, **87**, 569-588.

Murphy, J. R. (1998). Private communication.

Patton, H. J. and W. R. Walter (1994). Private communication.

Rodgers, A. J., W. R. Walter, C. A. Schultz, S. C. Meyers, and T. Lay (1999). A comparison of methodologies for representing path effects on regional P/S discriminants, *Bull. Seism. Soc. Am.*, 89, 394-408.

Sereno, T.J. (1990). Attenuation of Regional Phases in Fennoscandia and Estimates of Arrival Time and Azimuth Uncertainty using Data Recorded by Regional Arrays, SAIC-90/1472, Science Applications International Corporation, San Diego, California.